PHYSICAL REVIEW B **67**, 193104 (2003)

Origin of current-induced forces in an atomic gold wire: A first-principles study

Mads Brandbyge,[1,*] Kurt Stokbro,[1] Jeremy Taylor,[1] José-Luis Mozos,[2] and Pablo Ordejón[2]
[1]*Mikroelektronik Centret (MIC), Technical University of Denmark, Bldg. 345E, DK-2800 Lyngby, Denmark*
[2]*Institut de Ciencia de Materials de Barcelona, CSIC Campus de la U.A.B., 08193 Bellaterra, Spain*

(Received 10 December 2002; published 20 May 2003)

We address the microscopic origin of the current-induced forces by analyzing results of first principles density functional calculations of atomic gold wires connected to two gold electrodes with different electrochemical potentials. We find that current induced forces are closely related to the chemical bonding, and arise from the rearrangement of bond charge due to the current flow. We explain the current induced bond weakening/strengthening by introducing bond charges decomposed into electrode components.

DOI: 10.1103/PhysRevB.67.193104 PACS number(s): 73.40.Jn, 66.30.Qa, 87.15.By

The failure of interconnects in integrated circuits is often due to directionally biased diffusion of atoms caused by the presence of an electric current (electromigration).[1] In recent years the prospect of electronic devices operating essentially on the atomic/molecular scale has gained significant interest,[2] and electromigration and current-induced conformational changes are important issues when downscaling electronic components to these sizes.[3] A single atom wide gold contact is among the simplest atomic scale conductors and therefore ideal for fundamental studies of the current-induced forces. It is remarkable that these systems can sustain voltages up to several volts before breaking.[4–6]

Our aim here is to uncover the microscopic origin of the current-induced bond weakening/strengthening in an atomic gold wire. We analyze state-of-the-art first principles calculations of the current-induced forces while other investigations have focused on the theoretical foundation of these forces.[7] Traditionally the microscopic origin of the current induced force on an atom is related to electrostatic forces and the momentum transfer by the electron flow, the so called electron wind force.[1] However it is not necessary to make such a division.[7] We find that the current-induced forces are rather linked to the redistribution of bond charge or overlap population in the system. By extending the concept of overlap population to a nonequilibrium system with two electrochemical potentials, we can rationalize the first principles results in terms of a simple two orbital interaction model.

We have performed our calculations within density functional theory (DFT).[8–10] We employ the TRANSIESTA program[10] which allows a full atomistic description of the scattering region and the electrodes. DFT has previously been used to describe the current-induced forces acting on single atoms,[11,12] molecules,[3] and an atom adsorbed on an nanotube.[13] Recently, the current-induced forces in atomic wires, and the resulting ‘‘embrittlement,’’ was addressed by more approximate theory.[14]

We consider a simple symmetric geometry consisting of three atoms connecting electrodes in both the (100) and (111) directions, see Fig. 1. The electrode-electrode distance is in both cases chosen to be 9.6 Å and the wire atoms are initially relaxed at zero bias. We choose this particular geometry since here the middle atom (2) can roughly be considered to have only two bonds, namely, to the left atom (1) and the right atom (3).

When the voltage is applied we observe a substantial redistribution of the electronic charge. At 0 V the wires have a net negative charge of about 0.2 excess electrons. About half of this resides on atom 2. At 2 V the excess electrons on atom 2 are almost halved. This charge redistribution results in an asymmetric voltage drop where the main drop is between the negative electrode and atom 2 (see Fig. 1).

In Fig. 2(a) we show the calculated bond forces for the (100)/(111) wires with atomic positions fixed at the relaxed values[15] obtained for zero bias. We find that the forces on the symmetric atoms 1 and 3 roughly follow each other, also beyond the linear bias regime.[7] We note that the order of magnitude and direction of the bond forces at 2 V are similar for (100)/(111) while the detailed behavior differs: the bond forces for the (100) wire stay linear up to 1 V and level off around 2 V while we observe an onset of the bond forces for (111) at 1 V. The magnitude of the bond forces of the order of 1–1.5 nN for 1–2 V is sizable compared to the force required to break a one-atom thick wire ~1.5 nN.[16]

Along with the bond force we also show the overlap population (OP) in Fig. 2(a). The OP is a measure of the

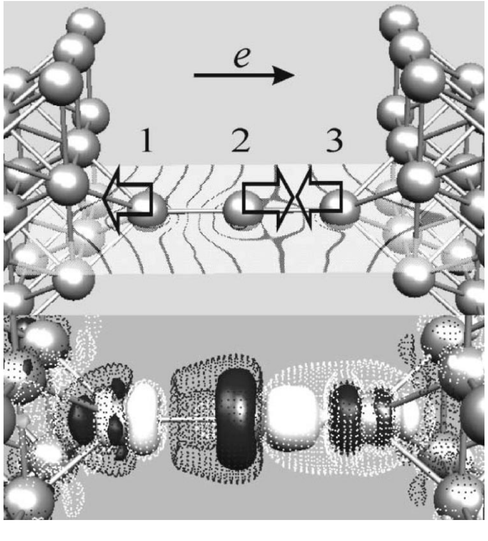

FIG. 1. (a) Direction of forces and voltage drop for the gold wire connecting (100) electrodes at 1 V bias. (b) Isodensity surfaces for the *change* in density from 0 to 1 V. Dark is deficit and white is extra electron density. The solid (dotted) surface correspond to $\pm 5\times 10^{-4} e/\text{Å}^3$ ($\pm 2\times 10^{-4} e/\text{Å}^3$).

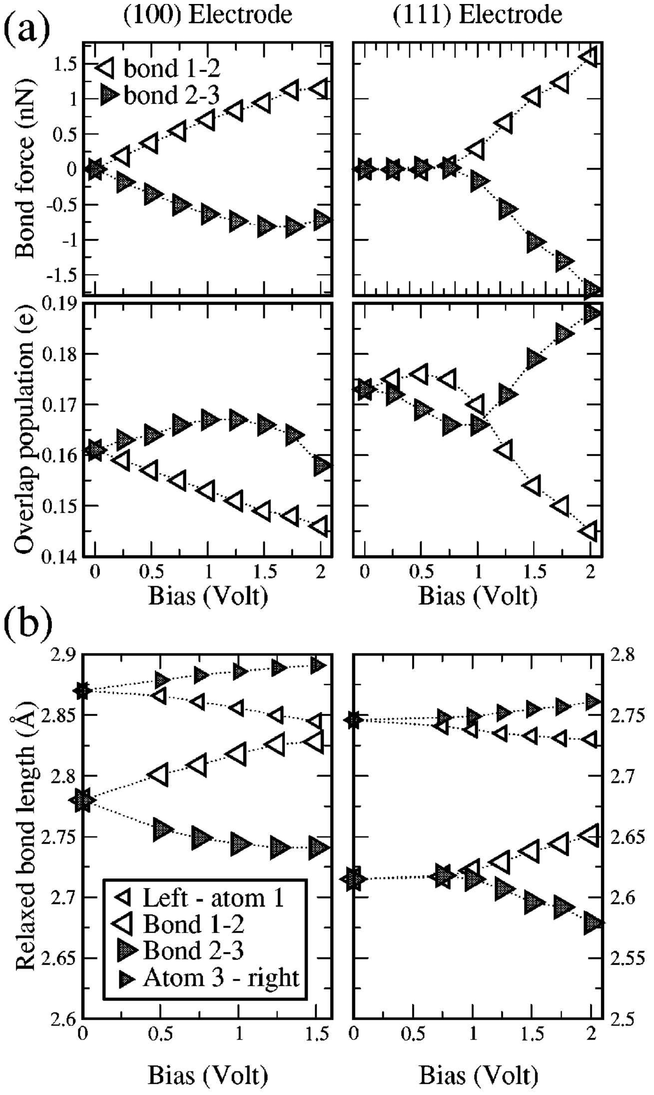

FIG. 2. (a) The bondforce and overlap(bond) population for the (100) and (111) connected wires. (b) The relaxed wire bondlengths for finite bias.

electronic charge residing in the bond. We note that except for the (111) wire at low bias, the force and OP curves are almost mirrored. The result that an increase (decrease) in bond charge makes the bond force compressive (repulsive) is what we expect intuitively. In Fig. 2(b) we show the bond lengths after subsequent relaxation of the wire atoms for finite bias. The main relaxations take place in the wire bonds with smaller displacements in the wire-electrode bonds.

We aim at an qualitative understanding of the results for the dependence of the force on the voltage bias. To this end we focus on the OP. We can express[17] the force acting on atom i due to the valence electrons using the force operator $\mathbf{F}_i$ and the density matrix $\mathbf{D}$,

$$\vec{F}_i = \mathrm{Tr}[\vec{\mathbf{F}}_i \mathbf{D}], \quad \text{where } \vec{\mathbf{F}}_i = -\frac{\partial \mathbf{H}}{\partial \vec{R}_i}. \tag{1}$$

Consider the bonding between two atoms represented by orbitals $|\phi_1\rangle$ and $|\phi_2\rangle$ and separated by bondlength b. From Eq. (1) we get the bond force,

$$F_{\text{bond}} = -2\left(\frac{\langle\phi_2|H'|\phi_1\rangle}{\langle\phi_2|\phi_1\rangle}\right)O_{12}, \quad H' = \frac{\partial H}{\partial b}, \tag{2}$$

where we assume that only the hopping element, $\langle\phi_2|H|\phi_1\rangle$, changes with b. The bond force is proportional to the OP for the 12 bond

$$O_{12} = 2\mathbf{S}_{12}\mathbf{D}_{12}. \tag{3}$$

The OP is typically taken as a simple measure of the strength of a chemical bond as suggested by Mulliken for molecules.[18] For extended systems the density matrix can be expressed in terms of the density of states (DOS) matrix, $\boldsymbol{\rho}$. In equilibrium we have

$$O_{12} = 2\mathbf{S}_{12}\int_{-\infty}^{\infty} d\varepsilon\, \boldsymbol{\rho}_{12}(\varepsilon)\, n_F(\varepsilon - E_F), \tag{4}$$

where n_F and E_F is the Fermi function and energy. The contribution from states at different energy(ε) in the extended system to the bonding between the two orbitals is described qualitatively by the OP weighted DOS (OPWDOS) or COOP curve $2\mathbf{S}_{12}\boldsymbol{\rho}_{12}(\varepsilon)$ as discussed by Hoffmann.[19]

Now we consider the nonequilibrium situation where an electrical current is running though a contact connecting two reservoirs, left and right (L, R), with different chemical potentials (μ_L, μ_R). The contact contains the 12 bond. In this case the bond force will change since the density and Hamiltonian matrices deviate from equilibrium values. The appropriate density matrix for the nonequilibrium situation is constructed from scattering states, and the total spectral density matrix ($\boldsymbol{\rho}$) is split into partial contributions corresponding to their left ($\boldsymbol{\rho}^L$) or right ($\boldsymbol{\rho}^R$) origin (see, e.g., Ref. 10),

$$\boldsymbol{\rho}(\varepsilon) = \boldsymbol{\rho}^L(\varepsilon) + \boldsymbol{\rho}^R(\varepsilon). \tag{5}$$

The density matrix for nonequilibrium is then found by filling the left and right originating states according to the respective chemical potentials[7,10]

$$\mathbf{D} = \int_{-\infty}^{\infty} d\varepsilon\, \boldsymbol{\rho}^L(\varepsilon)\, n_F(\varepsilon - \mu_L) + \boldsymbol{\rho}^R(\varepsilon)\, n_F(\varepsilon - \mu_R). \tag{6}$$

We split the overlap population(Eq. 4) further into its partial left and right components

$$O_{12} = O_{12}^L + O_{12}^R, \tag{7}$$

where

$$O_{12}^L = 2\mathbf{S}_{12}\int_{-\infty}^{\infty} d\varepsilon\, \boldsymbol{\rho}_{12}^L(\varepsilon)\, n_F(\varepsilon - \mu_L), \tag{8}$$

and likewise for R. When more orbitals are involved on atom 1 and 2 the overlap populations can be broken down in orbital components. In this case each orbital overlap will contribute with different weight to the bond force according to their different force matrix elements H'. This complication, together with the neglect of change in H' with applied voltage, makes the bond force and OP only roughly proportional,

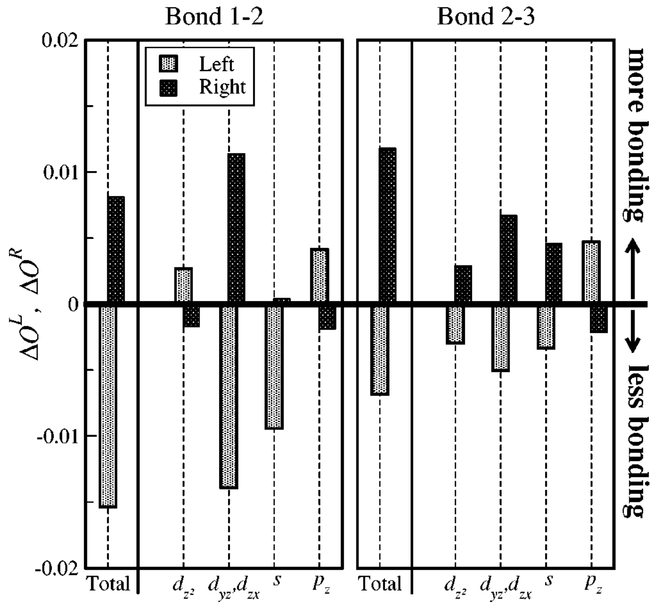

FIG. 3. The change in left and right partial OP, $\{O^L_{12},O^R_{12}\}$ and $\{O^L_{23},O^R_{23}\}$ for a change in bias from 0 to 1 V for the (100) wire. These are broken into main orbital contributions with respect to the middle atom (2). We show the sum of the contributions for the degenerate d_{yz} and d_{zx}.

as we observe for the gold wires in Fig. 2. However, as a first approximation, we can explain the observed change in bond forces from the change in OP, which in turn means the change in left (ΔO^L) and right (ΔO^R) contributions.

In Fig. 3 we consider the change from 0 V to 1 V in left and right OP of the 12 and 23 bonds for the (100) case [we see a quite similar pattern for (111)]. For both bonds ΔO^L is negative (decreasing bonding) while ΔO^R is positive (increasing bonding). We have resolved these further into the orbitals on atom 2 and display the main contributions in Fig. 3.

In order to understand the physics involved we present in Fig. 4(a) a simple picture. In the presence of current the electrons from the left electrode populate states above the original Fermi energy E_F. These populate bonding or antibonding states depending on the position of E_F. Likewise there is an depopulation in electrons from the right. To make this picture more explicit we consider in Fig. 4(b) a single bond between two atoms each with a single atomic level ε_L and ε_R. The levels couple via a matrix element $t<0$, and an overlap $S>0$, and form bonding/antibonding orbitals ε_B and ε_A. The left and right atoms are coupled to left and right electrodes modeled by a level broadening Γ_L of the left level and Γ_R for the right. For this bond the resulting partial DOS due to the states originating from the left is

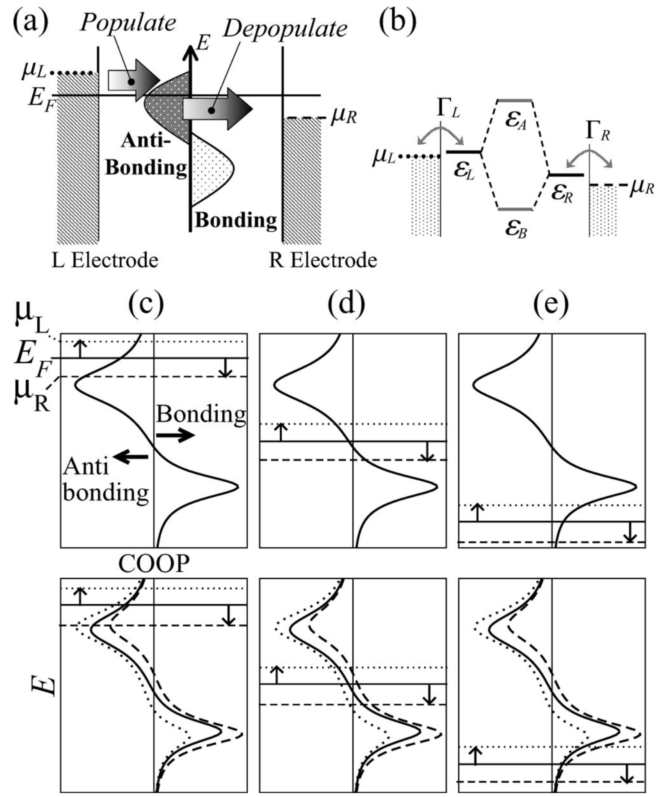

FIG. 4. (a) Generic picture of the COOP (x axis) curve and chemical potentials of the electrodes μ_L,μ_R deviating from the equilibrium $\mu_L=\mu_R=E_F$. (b) Simple model with a single bond between two atomic orbitals (ε_L, ε_R) forming bonding (ε_B) and antibonding states (ε_A). Atom L couples to the left electrode by Γ_L (life time $\hbar/\Gamma_L$) and likewise for atom R. (c)–(e) COOP curves for different initial filling factors. Left (right) quantities are denoted by dotted (dashed) lines; zero voltage quantities are solid. The top (bottom) panels represent zero (full) voltage drop between the atoms $\varepsilon_L=\varepsilon_R(\varepsilon_L-\varepsilon_R=\mu_L-\mu_R)$.

$$\rho^L(\varepsilon)=\frac{2}{\pi}\,\frac{\Gamma_L(\varepsilon_R-\varepsilon)(\varepsilon S+|t|)}{[(1-S^2)(\varepsilon-\varepsilon_A)(\varepsilon-\varepsilon_B)-\Gamma_L\Gamma_R]^2+[\Gamma_R(\varepsilon-\varepsilon_L)+\Gamma_L(\varepsilon-\varepsilon_R)]^2}. \tag{9}$$

We note that (i) ρ^R is found by exchanging $L\leftrightarrow R$. (ii) ρ^L is proportional to the coupling Γ_L, (iii) the crossover between bonding (positive) and antibonding (negative) is given by the position of ε_R. From (i), (iii) we see that ρ_L contains more antibonding character than ρ_R when $\varepsilon_L>\varepsilon_R$.

We have plotted L/R COOP curves in Figs. 4(c)–4(e) for different fillings and $\Gamma_L=\Gamma_R$. In the top row we assume that there is no voltage drop between the atoms $\varepsilon_L=\varepsilon_R$. Here the change in OP comes entirely from the change in filling due to the shift of μ_L and μ_R away from the equilibrium E_F [Eq.

(8)]. For almost filled states [Fig. 4(c), top] the lowering of μ_R deplete states with antibonding character and O^R increases. The increase in μ_L leads to a decrease in O^L which does not balance the increase in O^R. The net effect is a *decrease* in antibonding character and strengthening of the bond. When the states are almost empty [Fig. 4(e), top] we *also* observe a strengthening since now O^L increases more than O^R is decreasing. For a bond initially with maximal strength [Fig. 4(d), top] and, in general, for E_F located in a region where the COOP decreases, the bond weakens since both O^R and O^L decrease.

In the bottom row of Figs. 4(c)–4(e) we assume that the full voltage drop takes place between the two atoms $\varepsilon_L - \varepsilon_R = \mu_L - \mu_R > 0$. The bonding peak becomes dominating in the right COOP and likewise for the antibonding peak in the left COOP. The net result is less bond strengthening in (c) and (e), and more bond weakening in (d). The largest effect of a voltage drop is seen for half filling [Fig. 4(d), bottom], where a large negative ΔO_L occurs because the bonding peak decreases and at the same time more anti-bonding states are being occupied.

In summary, for equal coupling, $\Gamma_L = \Gamma_R$, our simple model yield (i) bond strengthening for almost empty/filled states, (ii) bond weakening for about half filled states, and (iii) a bond with a voltage drop is weaker than it would be without a drop. When the bond is not coupled equally well to left and right, $\Gamma_L \neq \Gamma_R$, the left and right overlap contributions have to be weighted accordingly.

In the case of the gold wires we can to a good approximation assume that the d_{yz}, d_{zx}, and p_z orbital on atom 2 only couple with the corresponding orbital on atom 1 and 3. The d_{yz}, d_{zx} states are almost filled and match the case in Fig. 4(c): $\Delta O^R > 0$ while $\Delta O^L < 0$. On the other hand the p_z states are almost empty and match the situation in Fig. 4(e): $\Delta O^L > 0$ while $\Delta O^R < 0$. This is exactly the behavior we observe in Fig. 3. For the *s* orbitals, which are slightly more than half-filled, we can expect a decrease in O^L, which will be especially pronounced if a voltage drop takes place in the bond [see Fig. 4(d), bottom]. This is also what we observe for the 12 bond in Fig. 3.

Based on our simple model we see that the almost completely filled states (*d*) and slightly more than half-filled states (*s*) together yield a *decrease* in O^L and *increase* in O^R. Since bond 12 couple more to the left electrode the total change in O^L will be bigger than the change in O^R. This explains the bond weakening of bond 12. The opposite is the case for bond 23. Also the voltage drop taking place in bond 12 will weaken this bond with respect to bond 23.

In conclusion we have analyzed first principles calculations of the current-induced forces in an atomic gold wire. We have shown that the current-induced forces are due to a shift in the population of bonding and antibonding levels, and can be explained by examining the change in electrode decomposed bond charges (overlap population) with applied voltage. Although we have concentrated on a simple system the approach should apply to atomic scale conductors in general.

We acknowledge support from the Danish Research Councils (M.B. and K.S.), European Union (SATURN project), and MCyT (J.L.M. and P.O). We also thank the Ψ_k network and CEPBA for funding collaborative visits.

---

*Electronic address: mbr@mic.dtu.dk

[1] R. S. Sorbello, Solid State Phys. **51**, 163 (1998).

[2] C. Joachim, J. K. Gimzewski, and A. Aviram, Nature (London) **408**, 541 (2000).

[3] M. D. Ventra, S. T. Pantelides, and N. D. Lang, Phys. Rev. Lett. **88**, 046801 (2002).

[4] G. R. Bollinger, H. E. van den Brom, N. Agraït, and J. M. van Ruitenbeek, Nature (London) **395**, 783 (1998).

[5] S. K. Nielsen, M. Brandbyge, E. Laegsgaard, I. Stensgaard, and F. Besenbacher, Appl. Phys. Lett. **77**, 708 (2000).

[6] M. Brandbyge, K. Hansen, K. Stokbro, J. M. van Ruitenbeek, and F. Besenbacher, Phys. Rev. Lett. **89**, 066804 (2002).

[7] T. N. Todorov, J. Hoekstra, and A. P. Sutton, Philos. Mag. B **80**, 421 (2000).

[8] We employ the SIESTA package (Ref. 9) extended to the nonequilibrium situation by the TRANSIESTA method (Ref. 10).

[9] E. Artacho, J. D. Gale, A. Garcia, J. Junquera, P. Ordejón, and D. Sánchez-Portal, J. Phys. C **14**, 2745 (2002).

[10] J. L. Mozos, P. Ordejón, J. Taylor, and K. Stokbro, Phys. Rev. B **65**, 165401 (2002).

[11] N. D. Lang, Phys. Rev. B **45**, 13 599 (1992).

[12] N. Kobayashi, K. Hirose, and M. Tsukada, Surf. Sci. **345**, 299 (1996).

[13] N. Mingo, L. Yang, and J. Han, J. Phys. Chem. B **105**, 11142 (2001).

[14] T. N. Todorov, J. Hoekstra, and A. P. Sutton, Phys. Rev. Lett. **86**, 3606 (2001).

[15] The force is less than 0.02 nN on all wire atoms.

[16] S. R. Bahn, N. Agraït, K. W. Jacobsen, and S. Vieira, Phys. Rev. Lett. **87**, 026101 (2001).

[17] Terms which take into account incompleteness and nonorthogonality are included in pracsis, see P. Ordejon, E. Artacho, and J. M. Soler, Phys. Rev. B **53**, R10 441 (1996).

[18] R. S. Mulliken, J. Chem. Phys. **23**, 1833 (1955); **23**, 2343 (1955).

[19] R. Hoffmann, Rev. Mod. Phys. **60**, 601 (1988).